

SHORT REPORT

CT-like images of the sacroiliac joint generated from MRI using susceptibility-weighted imaging (SWI) in patients with axial spondyloarthritis

Dominik Deppe,¹ Kay-Geert Hermann,¹ Fabian Proft ,² Denis Poddubnyy,³ Felix Radny,¹ Mikhail Protopopov ,² Marcus R Makowski,⁴ Torsten Diekhoff ¹

To cite: Deppe D, Hermann K-G, Proft F, *et al.* CT-like images of the sacroiliac joint generated from MRI using susceptibility-weighted imaging (SWI) in patients with axial spondyloarthritis. *RMD Open* 2021;**7**:e001656. doi:10.1136/rmdopen-2021-001656

► Additional supplemental material is published online only. To view, please visit the journal online (<http://dx.doi.org/10.1136/rmdopen-2021-001656>).

Received 4 March 2021
Accepted 24 May 2021



© Author(s) (or their employer(s)) 2021. Re-use permitted under CC BY-NC. No commercial re-use. See rights and permissions. Published by BMJ.

¹Department of Radiology, Freie Universität Berlin, Berlin, Germany

²Department of Gastroenterology, Infectiology and Rheumatology, Charité Universitätsmedizin Berlin Campus Benjamin Franklin, Berlin, Germany

³Division of Gastroenterology, Infectious Diseases and Rheumatology, Charité Universitätsmedizin Berlin, Berlin, Germany

⁴Department of Radiology, Charité Universitätsmedizin Berlin, Berlin, Germany

Correspondence to

Dr Torsten Diekhoff;
torsten.diekhoff@charite.de

ABSTRACT

Background To analyse the added value of susceptibility-weighted imaging (SWI) compared with standard T1-weighted (T1) MRI for detecting structural lesions of the sacroiliac joint (SIJ) in patients with axial spondyloarthritis (axSpA) using CT as reference standard.

Material and methods Sixty-eight patients with suspected or proven axSpA underwent both MRI and CT of the SIJ on the same day. Two readers separately scored CT, T1 and SWI for the presence of erosions, sclerosis and joint space changes using an established 24-region SIJ model. Disagreement was resolved by a third reader. Diagnostic accuracy (McNemar test), Cohen's kappa (k), sensitivity (SE) and specificity were calculated on the joint level using CT as reference.

Results In CT, 38 joints showed erosions, 67 sclerosis and 37 joint space changes. Agreement with CT for erosions was 92.6% (k=0.811 (0.7–0.92)) in SWI and 87.5% (k=0.682 (0.54–0.82)) in T1 (p=0.143) and agreement for sclerosis 84.6% (k=0.69 (0.57–0.81)) and 62.5% (k=0.241 (0.13–0.35)) (p<0.001), respectively. This resulted in superior SE of SWI (81.6% vs 73.7%) for erosions and sclerosis (74.6% vs 23.9%) at a minor expense of SP. No differences were detected for joint space changes.

Conclusion In patients with axSpA, SWI depicts erosions and sclerosis more accurately than T1 spin echo MRI at 1.5 T.

INTRODUCTION

Detection of structural damage of the sacroiliac joint (SIJ) including erosions, sclerosis and joint space changes is crucial for establishing the diagnosis of axial spondyloarthritis (axSpA) and monitoring disease progression. The modified New York Criteria include these structural changes in radiography but do not incorporate MRI.¹ Conversely, the Assessment of SpondyloArthritis international Society criteria incorporate osteitis in MRI for classification but attach less weight to structural lesions.^{1–3} While conventional sequences have recently been shown to detect

Key messages

- Susceptibility-weighted imaging (SWI) depicted erosion and sclerosis more accurately compared with T1-weighted MRI.
- SWI does not improve the detection of joint space changes.
- SWI allows the direct depiction of the cortical bone in the SIJ and its structural damages and create a CT-like MRI.
- By adding SWI to the standard protocol, structural damages could be detected more precisely in patients with axial spondyloarthritis which is important for differential diagnosis.

erosions with high diagnostic accuracy,⁴ standard MRI is limited because it cannot depict cortical bone directly (it is hypointense in all sequences) but relies on the contrast of bone, bone marrow and cartilage. Conversely, radiography and CT depict the bone directly due to X-ray attenuation of bone but involve radiation exposure and do not capture active inflammation, which is deemed important for early diagnosis but less specific for differential diagnosis.

There are some developments in MRI for direct bone depiction. One of them, susceptibility-weighted imaging (SWI),⁵ has been successfully applied to erosion detection in patients with peripheral arthritis.⁶ SWI depicts calcium structures directly by detecting and quantifying small magnetic field inhomogeneities surrounding calcium atoms. While SWI has been standard in many brain MRI protocols for several years, its transfer to musculoskeletal imaging was rather recent.⁷ Inversion of these images creates the impression of CT images in MRI.

The aim of our study was to investigate SWI in detecting structural SIJ damage in patients

with axSpA compared with T1-weighted (T1) sequences and using CT as standard of reference.

METHODS

Patients

We prospectively included 75 patients with suspected or diagnosed axSpA examined between February 2018 and November 2019. They were referred by the local rheumatology department either to confirm axSpA in patients with inflammatory back pain and other typical features of axSpA or to evaluate inflammatory activity in patients with an established diagnosis. The final diagnosis was made by the rheumatologist. Exclusion criteria were contraindications to MRI (eg, pacemaker), claustrophobia and pregnancy.

Imaging

All patients underwent MRI at 1.5 T. The protocol included conventional T1-weighted (T1) and STIR sequences and an SWI sequence of the SIJ acquired with 4mm slice thickness and 10% gap between slices in oblique coronal orientation (online supplemental file 1). CT was performed on the same day as dual-energy CT (DECT) on a single-source scanner (Canon Aquilion One Vision) and served as standard of reference. DECT source data were reconstructed in 120-equivalent blended images (equivalent to conventional CT) and reformatted to 3mm oblique coronal image stacks.

Image reading

Standard MRI (T1, STIR), SWI and CT of the SIJ were anonymised separately using Horos (The Horos Project, V.3.3.6, Pureview, Maryland, USA). Inverted SWI was viewed to imitate the impression of CT. The images were scored separately by two readers (reader 1: musculoskeletal radiologist with 11 years of experience; reader 2: research student with 2 years of experience). Disagreement was solved by an expert adjudicator (reader 3: musculoskeletal radiologist with 21 years of experience). Images were scored using a 24-region approach for erosions and sclerosis previously established by our group.⁸ Briefly, this model divides each SIJ into four quadrants and each quadrant into an anterior, central and posterior region. Joint space changes were scored per joint and region. Scores were as follows: 0–3 for erosions (0 no erosions, 1 small isolated erosions (n=1–2), 2 definite erosions (n=3–5; <3mm), 3 multiple (n>5) or confluent erosions); 0–2 for sclerosis (0 no sclerosis, 1 minor sclerosis (5–9mm), 2 evident sclerosis (≥10mm)); and 0–4 for joint space changes (0 normal joint space, 1 possible widening/narrowing, 2 definite widening/narrowing, 3 partial ankylosis, 4 complete ankylosis). Scoring results were reported using an in-house developed online electronic Case Report Form (eCRF). Readers 1 and 2 scored 10 standard MRI and CT test cases before the study reading.

Data analysis

Erosions, sclerosis and joint space changes were defined as positive if a score of 2 or higher was assigned per joint by both readers. Any disagreement was resolved by the third reader. Sum scores were separately calculated for each joint and reader. The mean of both readers' sum scores was calculated for each lesion in T1 and SWI for comparison with CT using Pearson's r. Sensitivity (SE), specificity (SP) and likelihood ratios (LR+ and LR–) were calculated for each MRI protocol and each lesion. Diagnostic accuracy was calculated for each lesion in SWI and T1 using CT as reference, and the results were compared with a McNemar test. Cohen's kappa (k) was calculated for agreement with CT and for interrater reliability. Statistical analysis was performed using SPSS (V.27.0.0.0).

RESULTS

Patients

Seven of 75 patients were excluded from analysis because they did not undergo MRI (known claustrophobia n=2, cancelled MRI due to claustrophobia n=2, cancelled MRI due to back pain n=1, possible pregnancy n=1) or CT (technical error n=1). Further patient characteristics are presented in [table 1](#).

Image reading and data analysis

Contingency tables, SE (SE), SP, LR and diagnostic accuracy data for the three types of structural lesions are compiled in [table 2](#). Imaging examples are presented in [figure 1](#).

Erosions

Thirty-eight joints were considered positive for erosions in CT, 35 in T1 and 34 in SWI. The sum score (average of both readers) was 2.05±3.37 in CT, 1.48±2.0 in T1 and 2.37±3.39 in SWI. Correlation with CT was moderate for T1 (r=0.786) and very strong for SWI (r=0.87). Diagnostic accuracy results including Cohen's kappa for agreement with CT are presented in [table 2](#). Inter-rater reliability was substantial for CT (k=0.741 (0.61–0.87); p<0.001), slight for T1 (k=0.185 (0–0.38); p<0.001) and moderate for SWI (k=0.424 (0.3–0.62); p<0.001).

Sclerosis

For sclerosis, 67 joints were scored positive in CT, 16 in T1 and 55 in SWI. The mean sum score for sclerosis was 2.87±3.09 in CT, 0.88±1.62 in T1 and 3.9±4.36 in SWI. Correlation with CT was moderate for T1 (r=0.677) and very strong for SWI (r=0.855). For diagnostic accuracy see [table 2](#). Inter-rater reliability for the presence of sclerosis was moderate for CT (k=0.569 (0.44–0.7); p<0.001), substantial for T1 (k=0.701 (0.51–0.89); p<0.001) and fair for SWI (k=0.394 (0.25–0.55); p<0.001).

Joint space changes

Joint space changes were considered to be present in 37 joints in CT, 33 in T1 and 38 in SWI. The mean sum score for this change was 2.26±3.26 in CT, 1.58±2.65 in

Table 1 Patient characteristics

	All patients	Patients with inflammatory disease (n=40)	Patients with non-inflammatory disease (n=28)
Sex	41.2% female (28/68)	27.5% female (11/40)	60.71% female (17/28)
Age	40.54±12.23	39.85 (SD 12.23)	41.54 (SD 11.96)
HLA-B27 positivity	55.8% (29/52)	73.33% (22/30)	21.82% (7/22)
Mean CRP	12.34 (n=24)	14.89 (SD 17.78; n=15)	7.58 (SD 18.38; n=9)+negative in 3 patients
BASDAI	4.67±1.61 (n=33)	4.6 (SD 1.61; n=27)	5.02 (SD 1.61; n=6)
Modified New York Criteria positivity	N/A	52.5% (21/40)	N/A
ASAS MRI criteria positivity	N/A	52.5% (21/40)	N/A
Erosion sum score	2.05 (SD 3.37)	3.16 (SD 3.37)	0.46 (SD 3.29)
Sclerosis sum score	2.87 (SD 3.09)	3.26 (SD 3.09)	2.31 (SD 3.03)
Joint space sum score	2.26 (SD 3.26)	3.53 (SD 3.26)	0.45 (SD 3.24)

Patient characteristics are presented for all patients and by subgroup according to the rheumatologist's final diagnosis (inflammatory vs non-inflammatory disease) by the rheumatologist. Inflammatory conditions were axial spondyloarthritis (axSpA) (n=35; r-axSpA: n=29, nr-axSpA: n=6), psoriatic arthritis with axial inflammation (n=4) and SAPHO (n=1). Non-inflammatory conditions were degenerative spine disease (n=14), osteitis condensans ilii (n=13) and psoriatic arthritis without axial involvement (n=1). The sum scores are mean scores in CT. ASAS, Assessment of SpondyloArthritis international Society; BASDAI, Bath Ankylosing Spondylitis Disease Activity Index; CRP, C-reactive protein; SAPHO, synovitis, acne, pustulosis, hyperostosis and synovitis syndrome.

T1 and 2.03±2.71 in SWI. Correlation of MRI with CT for joint space changes was very strong with both protocols (r=0.832 for T1, r=0.814 for SWI). For diagnostic accuracy see table 2. Cohen's kappa for inter-rater reliability was substantial for CT (k=0.669 (0.54–0.8); p<0.001) and T1 (k=0.654 (0.5–0.8); p<0.001) and fair for SWI (k=0.327 (0.16–0.5); p<0.001).

DISCUSSION

This is the first study using SWI to create CT-like MR images for detection of structural SIJ lesions in axSpA. Our results show that SWI improves the detection of erosions and sclerosis as important structural lesions of the SIJ, in terms of both diagnostic accuracy and

Table 2 Cross table, sensitivity (SE), specificity (SP), likelihood ratio (LR) and diagnostic accuracy

Erosions	CT+	CT–	Diagnostic accuracy	Likelihood ratio	Intermodality
T1+	28	7	SE 73.68% 56.9%–86.6%	LR– 0.28	Agreement 87.5%
T1–	10	91	SP 92.86% 85.84%–97.08%	LR+ 10.32	Cohen's k 0.682 0.54–0.82
SWI+	31	3	SE 81.58% 65.67%–92.26%	LR– 0.19	Agreement 92.6%
SWI–	7	95	SP 96.94% 91.31%–99.36%	LR+ 26.65	Cohen's k 0.811 0.7–0.92
Sclerosis	CT+	CT–			
T1+	16	0	SE 23.88% 14.31%–35.86%	LR– 0.76	Agreement 62.5%
T1–	51	69	SP 100.0% 94.79%–100.0%	LR+	Cohen's k 0.241 0.13–0.35
SWI+	50	5	SE 74.63% 62.51%–84.47%	LR– 0.27	Agreement 84.6%
SWI–	17	64	SP 92.75% 83.89%–97.61%	LR+ 10.30	Cohen's k 0.69 0.57–0.81
Joint space changes	CT+	CT–			
T1+	26	7	SE 70.27% 53.02%–84.13%	LR– 0.32	Agreement 86.8%
T1–	11	92	SP 92.93% 85.97%–97.11%	LR+ 9.94	Cohen's k 0.654 0.5–0.8
SWI+	28	10	SE 75.68% 58.8%–88.23%	LR– 0.27	Agreement 86%
SWI–	9	89	SP 89.9% 82.21%–95.05%	LR+ 7.49	Cohen's k 0.65 0.51–0.79

All values were calculated using CT as standard of reference or in comparison with CT (absolute agreement and Cohen's kappa). Agreement of SWI with CT was significantly higher for sclerosis (p<0.001) and tended to be higher for erosions (p=0.143), while there was no difference for joint space changes (p=1).

Bold text have been used to mark the subsection headings of the table. SWI, susceptibility-weighted imaging.

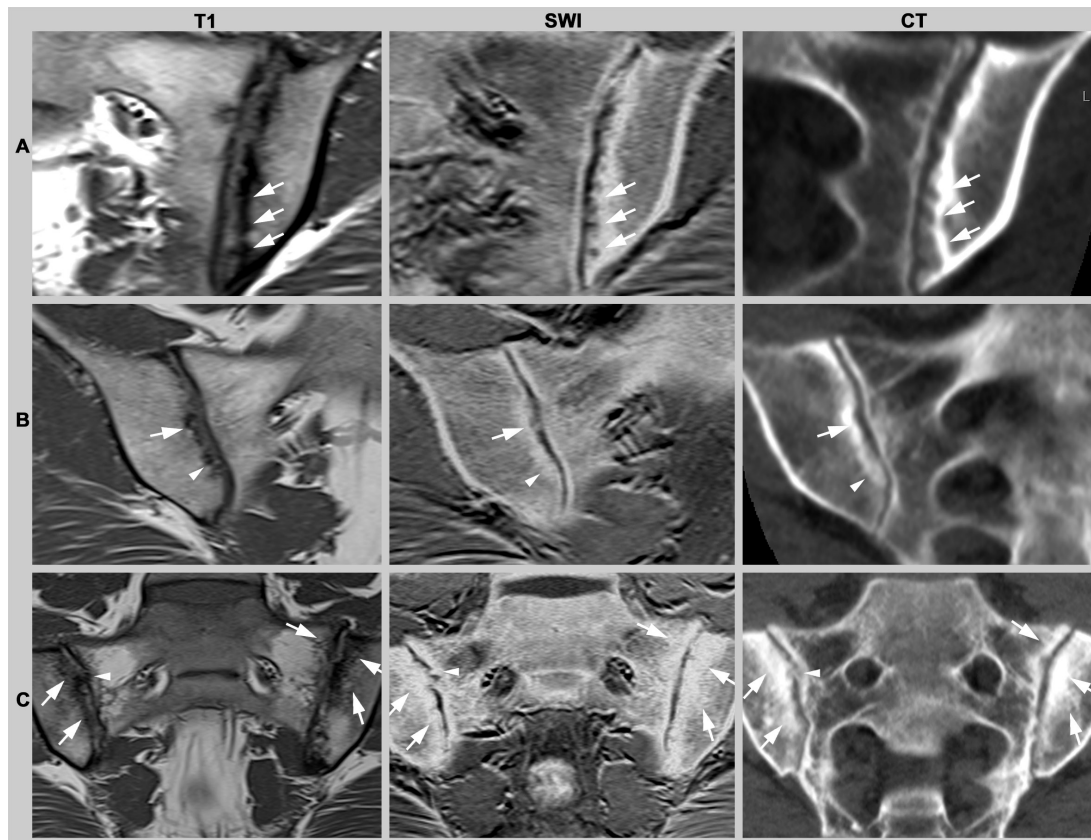


Figure 1 Illustration of structural changes of the sacroiliac joint in T1-weighted MRI, susceptibility-weighted imaging (SWI) and CT. Presented are inverted magnitude images of SWI, which are closest in appearance to conventional CT. (A) Right sacroiliac joint of a 28-year-old woman with axial spondyloarthritis. While T1 shows confluent erosions, single erosions are more clearly identified and delineated in SWI and CT (arrows). (B) False positive detection of erosion (arrow) in T1 in the left sacroiliac joint of a 51-year-old woman with spondylarthritis. SWI and CT show smooth joint surfaces with mild sclerosis mimicking erosive changes in T1 (arrowhead). (C) Subchondral sclerosis of both sacroiliac joints in a 28-year-old man with axial spondyloarthritis. The extent and severity of sclerosis are more clearly depicted on SWI compared with T1. Furthermore, new bone formation (bone buds) are also apparent in SWI but not in T1 (arrowhead).

correlation of sum scores. The detection of joint space alterations, however, is not improved by SWI compared with conventional MRI.

SWI has been shown to improve erosion depiction in patients with hand arthritis.⁶ While other novel MRI sequences such as volumetric interpolated breath-hold examination (VIBE) and MRI-based synthetic CT have been shown to be superior to T1 in detecting erosions in the SIJ,^{9–11} they do not allow direct visualisation of the cortical and trabecular bone structure and, thus, still suffer from typical MRI shortfalls. VIBE, for example, is a gradient echo sequence with an undesired T2* effect that causes a signal loss in the vicinity of calcium crystals, resulting in the typical stark contrast of soft tissue and bone. Conversely, SWI exploits the paramagnetic characteristics of calcium and the resulting T2* effect directly for improved contrast in musculoskeletal imaging. While SWI is a widely available and commonly used pulse sequence in neuroimaging and can be easily transferred to musculoskeletal imaging, MRI-based synthetic CT needs specifically trained AI software. Further developments in SWI have been used to directly quantify materials, but this was not investigated in our study.¹²

SWI may have several advantages for clinical practise. Before the advent of SWI, evaluation of structural changes by direct depiction of cortical bone was only possible with imaging modalities using ionising radiation.¹³ A standard MRI protocol supplemented by SWI both provides diagnostic information on the presence of active bone marrow lesions (osteitis) and allows accurate detection of structural lesions in a single imaging session by adding 5min and 47s of scan time. This plays an important role when it comes to differential diagnosis or monitoring of disease progression.¹⁴ In MRI of the SIJ, an important differential diagnosis for the presence of osteitis is mechanical stress, for example, in osteitis condensans ilii. One factor that can help in differentiating these non-erosive conditions from axSpA is the absence of erosions in the presence of sclerosis.^{15,16} The latter is even more pronounced in SWI, but showed high specificity in our analysis.

Still, some limitations of this study have to be discussed. We included a mixed population of patients with and without axSpA. Ethical concerns prohibited inclusion of healthy controls due to the radiation exposure of CT. A statistically significant improvement was only shown

for sclerosis. Our results need to be verified in larger patient populations, for MRI at 3 T, and in comparison with other novel sequences (VIBE, MR-based synthetic CT) and thinner slices. Some clinical and laboratory data were not available for all patients. We provide a structural lesion analysis only and do not elaborate on the diagnostic impact of SWI.

In conclusion, SWI depicts erosions and sclerosis more accurately than T1-weighted spin echo MRI at 1.5 T and may provide useful additional information for the diagnosis of axSpA.

Twitter Mikhail Protopopov @mprotopopov

Acknowledgements The authors thank Bettina Herwig for language editing.

Contributors DD: patient acquisition, image scoring, data evaluation, statistical calculations, article draft, critical revision of the manuscript for important intellectual content. KGH: conception and design of the study, design of scoring system, image scoring, critical revision of the manuscript for important intellectual content. FP: patient acquisition, data collection, critical revision of the manuscript for important intellectual content. DP: patient acquisition, statistical calculations, critical revision of the manuscript for important intellectual content. MP: patient acquisition, critical revision of the manuscript for important intellectual content. MRM: conception and design of the study, critical revision of the manuscript for important intellectual content. TD: conception and design of the study, design of scoring system, image scoring, data evaluation, statistical calculations, critical revision of the manuscript for important intellectual content.

Funding TD received a research grant from the Assessment of Spondyloarthritis international Society. Other than that, the authors have not declared a specific grant for this research from any funding agency in the public, commercial or not-for-profit sectors.

Competing interests KGH reports personal fees from AbbVie, personal fees from Novartis, personal fees from Merck, personal fees from Pfizer, outside the submitted work. FP reports personal fees from AbbVie, personal fees from AMGEN, personal fees from BMS, personal fees from Celgene, personal fees from MSD, grants and personal fees from Novartis, personal fees from Pfizer, personal fees from Roche, grants and personal fees from UCB, outside the submitted work. DP reports grants and personal fees from AbbVie, personal fees from Bristol-Myers Squibb, grants and personal fees from Eli Lilly, grants and personal fees from MSD, grants and personal fees from Novartis, grants and personal fees from Pfizer, personal fees from Roche, personal fees from UCB, personal fees from Biocad, personal fees from GlaxoSmithKline, personal fees from Gilead, outside the submitted work. TD reports personal fees from Canon MS, MSD, Roche and Novartis and an institutional grant from Canon MS outside the submitted work.

Patient consent for publication Not required.

Ethics approval The study was approved by the Charité institutional review board under EA1/086/16 and all patients gave written informed consent. Authorisation by the Federal Office for Radiation Protection was waived.

Provenance and peer review Not commissioned; externally peer reviewed.

Open access This is an open access article distributed in accordance with the Creative Commons Attribution Non Commercial (CC BY-NC 4.0) license, which permits others to distribute, remix, adapt, build upon this work non-commercially, and license their derivative works on different terms, provided the original work is properly cited, appropriate credit is given, any changes made indicated, and the use is non-commercial. See: <http://creativecommons.org/licenses/by-nc/4.0/>.

ORCID iDs

Fabian Proft <http://orcid.org/0000-0003-4306-033X>

Mikhail Protopopov <http://orcid.org/0000-0003-4840-5069>

Torsten Diekhoff <http://orcid.org/0000-0003-3593-1449>

REFERENCES

- van der Linden S, Valkenburg HA, Cats A. Evaluation of diagnostic criteria for ankylosing spondylitis. A proposal for modification of the new York criteria. *Arthritis Rheum* 1984;27:361–8.
- Lambert RGW, Bakker PAC, van der Heijde D, *et al.* Defining active sacroiliitis on MRI for classification of axial spondyloarthritis: update by the ASAS MRI Working group. *Ann Rheum Dis* 2016;75:1958–63.
- Rudwaleit M, van der Heijde D, Landewe R, *et al.* The development of assessment of spondyloarthritis International Society classification criteria for axial spondyloarthritis (Part II): validation and final selection. *Ann Rheum Dis* 2009;68:777–83.
- Maksymowych WP, Lambert RGW, Østergaard M, *et al.* MRI lesions in the sacroiliac joints of patients with spondyloarthritis: an update of definitions and validation by the ASAS MRI Working group. *Ann Rheum Dis* 2019;78:1550–8.
- Bender YY-N, Diederichs G, Walter TC, *et al.* Differentiation of osteophytes and disc herniations in spinal radiculopathy using susceptibility-weighted magnetic resonance imaging. *Invest Radiol* 2017;52:75–80.
- Ulas ST, Diekhoff T, Hermann KGA, *et al.* Susceptibility-Weighted MR imaging to improve the specificity of erosion detection: a prospective feasibility study in hand arthritis. *Skeletal Radiol* 2019;48:721–8.
- Nörenberg D, Ebersberger HU, Walter T, *et al.* Diagnosis of calcific Tendonitis of the rotator cuff by using susceptibility-weighted MR imaging. *Radiology* 2016;278:475–84.
- Diekhoff T, Hermann K-GA, Greese J, *et al.* Comparison of MRI with radiography for detecting structural lesions of the sacroiliac joint using CT as standard of reference: results from the SIMACT study. *Ann Rheum Dis* 2017;76:1502–8.
- Diekhoff T, Greese J, Sieper J, *et al.* Improved detection of erosions in the sacroiliac joints on MRI with volumetric interpolated breath-hold examination (VIBE): results from the SIMACT study. *Ann Rheum Dis* 2018;77:1585–9.
- Baraliakos X, Hoffmann F, Deng X, *et al.* Detection of erosions in Sacroiliac joints of patients with axial spondyloarthritis using the magnetic resonance imaging volumetric Interpolated Breath-hold examination. *J Rheumatol* 2019;46:1445–9.
- Jans LBO, Chen M, Elewaut D, *et al.* MRI-Based synthetic CT in the detection of structural lesions in patients with suspected sacroiliitis: comparison with MRI. *Radiology* 2021;298:343–9.
- Liu C, Li W, Tong KA, *et al.* Susceptibility-Weighted imaging and quantitative susceptibility mapping in the brain. *J Magn Reson Imaging* 2015;42:23–41.
- Stal R, van Gaalen F, Sepriano A, *et al.* Facet joint ankylosis in r-axSpA: detection and 2-year progression on whole spine low-dose CT and comparison with syndesmophyte progression. *Rheumatology* 2020;59:3776–83.
- Weber U, Lambert RGW, Pedersen SJ, *et al.* Assessment of structural lesions in sacroiliac joints enhances diagnostic utility of magnetic resonance imaging in early spondylarthritis. *Arthritis Care Res* 2010;62:1763–71.
- Poddubnyy D, Weineck H, Diekhoff T, *et al.* Clinical and imaging characteristics of osteitis condensans ilii as compared with axial spondyloarthritis. *Rheumatology* 2020;59:3798–806.
- Hoballah A, Lukas C, Leplat C, *et al.* MRI of sacroiliac joints for the diagnosis of axial spa: prevalence of inflammatory and structural lesions in nulliparous, early postpartum and late postpartum women. *Ann Rheum Dis* 2020;79:1063–9.